Free-Flow Wind Speed Estimation for a Wind Turbine Affected by Wake

Eduardo B. R. F. Paiva[1,2], Olivier Lepreux[1], and Delphine Bresch-Pietri[2]

***Abstract*— We present a method to estimate the time-varying free-flow wind speed on a wind farm based on local wind speed measurements taken by a wind turbine inside the wake zone of a turbine array. Our approach relies on a simple modeling of the speed deficit as a 1-D transport equation [1]. We propose to estimate the free-flow wind speed by integrating the error between the local wind measurement and an estimation of it computed with the free-flow estimate. We provide a bound on the estimation error which we formally prove. Finally, we provide numerical simulations to illustrate the interest and the performance of the proposed method.**

I. Introduction

The wind energy installed capacity has been growing steadily in the recent past and is expected to continue to do so in the foreseeable future. By the end of 2021, the worldwide installed capacity was 837 GW, and more than 20% of it was added from the beginning of 2020 to the end of 2021 [2]. Wind turbines are now deployed in ever denser wind farms, which leads to challenges in the development of controllers for such structures since the proximity between wind turbines causes them to interfere with each other through aerodynamic interactions.

One of these aerodynamic effects is the speed deficit in the wake: a wind turbine creates behind itself a region where the wind is slower and more turbulent than the incoming wind that drives the turbine. When multiple turbines are close to each other, their wakes superpose in an intricate manner, and the downwind turbines experience a deteriorated wind condition compared to that of the upwind turbines and, consequently, generate less power. Furthermore, it is now well established in the wind energy literature that greedy approaches where each wind turbine is an isolated agent seeking to maximize its power output without considering its interactions with the other turbines are generally not optimal when one considers the entire farm power production as the objective function, see, e.g., [3]. In this context, the wind energy community has been proposing wind farm control strategies that take wake dynamics into account to improve the power production of a wind farm as a whole. A comprehensive review of the recent wind farm control literature is given by [4], shorter surveys are provided in [3], [5], and earlier works include [6], [7].

[1]Eduardo B. R. F. Paiva and Olivier Lepreux are with IFP Energies nouvelles, Rond-point de l'echangeur de Solaize, BP 3, 69360 Solaize, France {eduardo.bezerra-rufino-ferreira-paiva, olivier.lepreux}@ifpen.fr

[2]Eduardo B. R. F. Paiva and Delphine Bresch-Pietri are with Centre Automatique et Systèmes, MINES ParisTech, PSL, 60 bd Saint-Michel, 75006 Paris, France delphine.bresch-pietri@mines-paristech.fr

To employ wind farm control techniques and for monitoring purposes, though, one needs information about the wind acting on the wind farm. Ideally, one wants to have a real-time measurement of the free-flow wind speed, i.e., the wind speed without the effect of the turbines. However, one will often face a lack of sensors to obtain such measurements. Indeed, the anemometers with which wind turbines are normally equipped are well-suited only to provide a time-averaged measurement of the wind speed and this measurement is not exactly that of the effective wind speed, i.e., the speed that is correlated with power production, because the anemometer only gives a punctual measurement and is placed behind the rotor where the wind is affected by the presence of the turbine (see, e.g., [8] and references therein). Furthermore, better-suited tools such as a nacelle LiDAR (Light Detection and Ranging) sensor, see, e.g., [9], [10], are rarely available for all turbines in the wind farm due to cost reasons.

In this paper, we consider the case where one wants to estimate the free-flow wind speed but has access only to an effective wind speed measurement downwind from a turbine array, which we refer to as the local speed measurement. This could be the case, e.g., when this measurement is taken from a LiDAR sensor mounted on another turbine downwind from the array (for lack of access, a fault on the upwind turbine, or any other reason).

Estimation techniques such as the ones reviewed in [4] usually rely on nonlinear versions of the Kalman Filter that, whilst being regarded as powerful tools and yielding good results in many applications, do not have guaranteed performance.

The method we propose to apply relies on a simple 1-D model of the wake, initially proposed in [1], to describe the speed deficit caused by the wake of a turbine. Using an analytical solution to this model, we propose to estimate the local speed measurement based on a free flow estimate, which, in turn, is updated by simply integrating the error between the actual local speed measurement and its estimate. Furthermore, we provide mathematical guarantees of the performance of our method, under mild assumptions. This is the main contribution of the paper. Numerical simulations obtained with NREL's FAST.Farm [11], [12] confirm the interest of the proposed estimation methodology.

The rest of this paper is organized as follows. In Section II, we present the problem under consideration more formally and detail our proposed estimation approach, including a short exposition of the analytical wake model we adopt and a theorem quantifying a bound of the corresponding estimation

error. In Section III, we present and analyze numerical results to assess the effectiveness of our method. Finally, we present some concluding remarks in Section IV.

II. Problem Formulation and Proposed Approach

Consider an array of wind turbines aligned with the wind direction. We are interested in the situation where one wants to estimate the free-flow wind speed but only has access to local speed information measured downwind from this array by, e.g., a meteorological mast or another wind turbine. When the downwind element is another turbine, the effective wind speed (not considering the effect of this turbine itself) can be obtained, e.g., with a nacelle LiDAR sensor or by employing an estimation technique that infers the effective wind speed from the SCADA data available to the turbine. In any case, this local measurement is affected by the wake of the upwind turbines and, therefore, does not correspond to the free-flow wind speed. Fig. 1 shows a schematic of this situation, where the measurement device is a LiDAR sensor on a downwind turbine.

The problem addressed in this paper is to reconstruct the free-flow wind speed using only the aforementioned measurement.

To this end, we employ an estimation strategy that uses an analytical model of the wake to estimate the local measurement and feeds back the error between this estimate and the actual measurement to update the estimate of the free-flow wind speed. In the following subsections, we describe first the wake model we use and then the update law for the free-flow speed estimate together with a theorem that provides an evaluation of the performance of this method.

In the following subsections, we present the wake model we use, then the update law for the free-flow wind speed estimate, and the implementation of the method.

A. Wake model

We apply the model proposed in [1], which uses a 1-D first-order hyperbolic PDE to model the speed deficit caused by a wind turbine. This model was initially proposed for a constant free-flow speed, but it has since been applied also to the time-varying case [13].

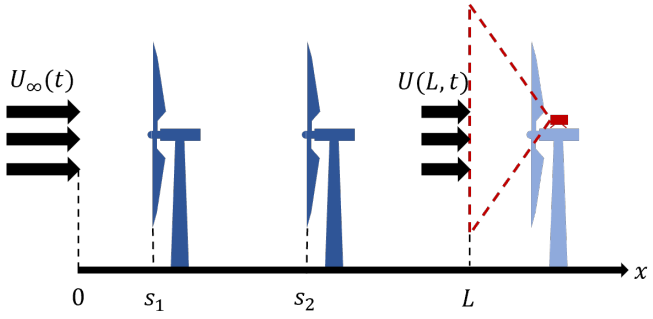

Fig. 1. Array of wind turbines and downwind measurement device. In this case, we have an array of two wind turbines and the measurement device is a LiDAR sensor mounted on the nacelle of a third turbine downwind from the relevant array.

Given an array of N wind turbines, this model characterizes the speed deficit caused by the ith one by

$$\frac{\partial \delta u_i}{\partial t} + U_\infty(t)\frac{\partial \delta u_i}{\partial x} = -w_i(x)U_\infty(t)\delta u_i(x,t) + S_i(x,t), \tag{1}$$

$$\delta u_i(0,t) = 0, \tag{2}$$

with

$$w_i(x) = \frac{2d_i'(x)}{d_i(x)}, \quad S_i(x,t) = \frac{2a_i U_\infty^2(t)}{d_i^2(x)}G_i(x), \tag{3}$$

$$d_i(x) = 1 + \kappa_i \ln\left(1 + \exp\left(\frac{x - s_i - D}{D/2}\right)\right), \tag{4}$$

$$G_i(x) = \frac{1}{(D/2)\sqrt{2\pi}} \exp\left(-\frac{(x-s_i)^2}{2(D/2)^2}\right). \tag{5}$$

Here, U_∞ is the free-flow wind speed (which is always positive), δu_i is the speed deficit caused by the ith turbine in the array, $\kappa_i > 0$ is a coefficient related to the wake diameter expansion, $a_i > 0$ is the induction factor of the ith turbine[1], $D > 0$ is the rotor diameter (assumed the same for all turbines), and $s_i > 0$ is the x position of the ith turbine. For convenience, we label the turbines so that $s_1 < s_2 < \ldots < s_N$. It should be noted that the boundary of the domain should be far upwind from the turbine array, i.e., $s_1 \gg 0$. We denote by L the x position where the wind speed is measured.

We can express the solution to (1)-(2), for $x \in [0, L]$ and $t > 0$, as[2]

$$\delta u_i(x,t) = \frac{2a_i}{d_i^2(x)} \int_0^x G_i(\xi) U_\infty(t - \tau(x-\xi, t))d\xi, \tag{6}$$

where τ is a delay implicitly defined by

$$\int_{t-\tau(x,t)}^{t} U_\infty(r)dr = x. \tag{7}$$

This integral equation uniquely defines the delay $\tau(x,t)$, which is referred to as transport delay [15] or hydraulic delay [16]. Note that this integral relation corresponds to the integration along the characteristic lines of (1).

In the estimation technique that we use later in the paper, we make a simplification with respect to the original model [1]. Namely, we use a simple linear superposition of the speed deficits to compute the wind speed, i.e., the wind speed U at any point of the domain is computed as

$$U(x,t) = U_\infty(t) - \sum_{i=1}^{N} \delta u_i(x,t). \tag{8}$$

Note that the literature proposes different ways to superpose the wakes of multiple turbines [17]. Here, we choose the simplest linear relation as it is more convenient to handle but is also reported in [18] as delivering a satisfactory result.

We assume we can write the measured output as

$$y(t) = U(L,t) + \Delta(t), \tag{9}$$

[1]We assume each induction factor to be constant throughout the time window of interest.

[2]Refer to [14] for details on how to obtain this solution.

where Δ is a term representing modeling errors and measurement noise. Indeed, the exact and complex behavior of the wake phenomenon cannot be entirely captured by the simplified model presented above. For this reason, we explicitly account for a model error by this additive term in the measurement equation. Note that wake modeling itself is an active area of research with extensive literature but beyond the scope of this paper, a couple of reviews that the interested reader may refer to are [19], [20].

Moreover, we make the following assumptions:

Assumption 1: There exist constants $U_m > 0$ and $\zeta \geq 0$ such that $U_\infty(t) \geq U_m$ and $|\dot{U}_\infty(t)| \leq \zeta$ for all $t \in \mathbb{R}$.

Assumption 2: There exists a constant $\Delta_M \geq 0$ such that $|\Delta(t)| \leq \Delta_M$ for all $t \in \mathbb{R}$.

Assumption 3: For $i = 1, \ldots, N$ define

$$\alpha_i = \frac{2a_i}{d_i^2(L)} \int_0^L G_i(\xi) d\xi, \tag{10}$$

$$\beta_i = \frac{2a_i}{d_i^2(L)} \int_0^L (L - \xi) G_i(\xi) d\xi. \tag{11}$$

We have

$$Z \triangleq \sum_{i=1}^{N} \left(\alpha_i + \frac{\beta_i \zeta}{U_m^2} \right) < 1 \text{ and } \frac{\Delta_M}{1 - Z} < U_m. \tag{12}$$

Assumption 1 requires the free-flow to be lower-bounded by a positive constant, which, in turn, ensures that the transport delay defined in (7) is upper-bounded. This and the fact that the variations of the free-flow and the error Δ are bounded, as required by Assumption 2, are reasonable requirements from a practical point of view.

Assumption 3 is the most demanding and technical one. It requires the measurement error to be sufficiently small for our estimation technique to work, as it is based on the simplified wake model (1)-(2). Furthermore, it also requires $Z < 1$. This originates from the use of Halanay's inequality in our stability proof, as will be detailed in the sequel.

We now turn our attention to the proposed estimation strategy.

B. Free-flow wind speed estimation method

Let $\hat{U}_\infty(t)$ represent the estimate of the free-flow wind speed at time t. Similarly, define the estimate of the measured output at time t, $\hat{y}(t)$, as

$$\hat{y}(t) = \hat{U}_\infty(t) - \sum_{i=1}^{N} \delta \hat{u}_i(t), \tag{13}$$

where

$$\delta \hat{u}_i(t) = \frac{2a_i}{d_i^2(L)} \int_0^L G(\xi - s_i) \hat{U}_\infty(t - \hat{\tau}(L - \xi, t)) d\xi \tag{14}$$

and $\hat{\tau}$ is defined by the relation

$$\int_{t - \hat{\tau}(x,t)}^{t} \hat{U}_\infty(r) dr = x. \tag{15}$$

Note that (14) and (15) are the counterparts of (6) and (7), respectively, but with the estimated free-flow wind speed $\hat{U}_\infty$ instead of the actual one, U_∞. Furthermore, we define the error variables

$$\tilde{U}_\infty(t) = U_\infty(t) - \hat{U}_\infty(t), \tag{16}$$

$$\delta \tilde{u}_i = \delta u_i(L, t) - \delta \hat{u}_i(t). \tag{17}$$

We propose to update the free-flow speed estimate using the following rule for $t > 0$:

$$\dot{\hat{U}}_\infty(t) = k(y(t) - \hat{y}(t)), \tag{18}$$

where $k > 0$ is a constant gain to be designed. As (14)-(15) use past values of $\hat{U}_\infty$, we use $\hat{U}_\infty(t) = \hat{U}_\infty(0) \geq U_m$ for all $t \leq 0$.

We can then establish the following result.

Theorem 1: Consider the system (1)-(2) satisfying Assumptions 1, 2, and 3 and the free-flow wind speed estimate $\hat{U}_\infty$ defined according to (13)-(18). Then, there exist $\hat{U}_m \in (0, U_m - \Delta_M/(1 - Z))$ and $k_* > 0$ such that, if $k > k_*$ and $\sup_{s \in [-\bar{\tau}, 0]} |\tilde{U}_\infty(s)| \leq U_m - \hat{U}_m - \Delta_M/(1 - Z)$, then $\hat{U}_\infty(t) \geq \hat{U}_m$ for all $t \geq 0$ and there exists $\sigma > 0$ such that

$$|\tilde{U}_\infty(t)| \leq \sup_{s \in [-\bar{\tau}, 0]} |\tilde{U}_\infty(s)| e^{-\sigma t} + \frac{\zeta}{k(1 - Z)} + \frac{\Delta_M}{1 - Z}. \tag{19}$$

Proof: See the Appendix. ∎

Notice Theorem 1 states that the steady-state error is bounded by the sum of two terms. The first one is related to ζ and we can make it arbitrarily small by choosing a large gain k. The second one is related to the modeling error and is not affected by the choice of the gain.

According to this result, one should thus adapt the update gain k according to the magnitude of the free-flow variations: the more important they are, the larger the gain should be, to faster counteract them. It is also worth underlining that Theorem 1 requires to bound the initial estimation error. This technical assumption does not seem to be so restrictive in practice as the simulations detailed in the sequel illustrate. Future works should focus on alleviating this assumption.

C. Implementation

Here, we detail the implementation of the proposed method. We propose to use a first-order discretization with a fixed time-step of the time-integral formulation of the solution to (1)-(2), which is

$$\delta u_i(x, t) = \frac{2a_i}{d_i^2(x)} \int_{t - \tau(x,t)}^{t} G_i(x - \Lambda(s, t)) U_\infty^2(s) ds, \tag{20}$$

with

$$\Lambda(s, t) = \int_s^t U_\infty(r) dr. \tag{21}$$

We use this form of the solution rather than the space-integral formulation presented before as it is easier to implement since computing (6) would require computing the transport delay for each iteration of the integration loop. This is avoided in this case as explained below.

Algorithm 1 shows the pseudo-code for the implementation. We use square brackets to denote the arguments in discrete time, so, for instance, $y[n] = y(n\Delta t)$, where Δt is the time-step. Recall that we assume the free-flow wind

speed estimate is constant before the estimation procedure starts running, i.e., if $j \leq 0$, we use $\hat{U}_\infty[j] = \hat{U}_\infty(0)$.

Notice that the estimation procedure might use a time step smaller than the time step used to obtain the measurements. This may be a feature of interest to mitigate the steady-state error as, according to Theorem 1, this may require using a high value for the gain k, which, in general, requires using a small Δt. In this case, we simply interpolate the measurements using a zero-order holder. Also, we include saturation in the update law implementation so that the free-flow speed estimate remains lower-bounded even with the numerical errors that may be originated from the discretization.

Moreover, note that the "while loop" is used to perform the integral operation in (20). The condition $\hat{\Lambda} < L$ is used because $\Lambda(t - \tau(L,t),t) = L$, thus, we can stop the integration at the correct bound without computing the value of transport delay in advance.

Most of the computational cost comes from the computation of the speed deficits. If the free-flow wind speed estimate is nearly constant, we can roughly say that the computational time for each iteration of the outermost loop is $O(N/\Delta t)$.

In terms of memory usage, we need to store the values $\hat{U}_\infty$ in between iterations of this outermost loop. Since $\hat{U}_\infty \geq \hat{U}_m$, the number of iterations of the "while loop" is limited and we need at most $\lfloor L/(\hat{U}_m \Delta t) \rfloor + 1$ past values of $\hat{U}_\infty$.

Algorithm 1 Implementation of the proposed method

for $n = 0, 1, 2, \ldots$ **do**
  $j \leftarrow n$, $\hat{u}_i \leftarrow 0$, $\hat{\Lambda} \leftarrow 0$
  for $i = 1, \ldots, N$ **do**
    $\delta\hat{u}_i[n] \leftarrow 0$
  end for
  while $\hat{\Lambda} < L$ **do**
    for $i = 1, \ldots, N$ **do**
      $\delta\hat{u}_i[n] \leftarrow \delta\hat{u}_i[n] + \frac{2a_i}{d_i^2(L)} G_i(L - \hat{\Lambda})\hat{U}_\infty^2[j]\Delta t$
    end for
    $\hat{\Lambda} \leftarrow \hat{\Lambda} + \hat{U}_\infty[j]\Delta t$
    $j \leftarrow j - 1$
  end while
  $\hat{y}[n] \leftarrow \hat{U}_\infty[n] - \delta\hat{u}_1[n] - \ldots - \delta\hat{u}_N[n]$
  $\hat{U}_\infty[n+1] \leftarrow \max\left\{\hat{U}_\infty[n] + k(y[n] - \hat{y}[n])\Delta t, \hat{U}_{min}\right\}$
end for

III. Numerical Results

To assess the performance of the method, we tested it using NREL's FAST.Farm simulator [11], [12] to play the role of the actual wind farm and provide us with the speed measurement.

We use a configuration where we have an array of three turbines evenly spaced $5D$ apart and the first turbine is at $s_1 = 5D$. We tested two cases. In the first one, we consider we can measure the effective wind speed for the second turbine, so $N = 1$ and $L = 10D$. In the second case, we measure the effective wind speed of the third turbine, so $N = 2$ and $L = 15D$. In all simulations, the turbines used are NREL's 5 MW turbine model with a rotor diameter of $D = 126$ m.

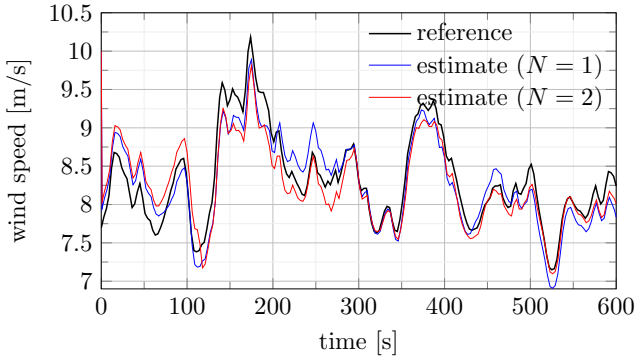

Fig. 2. Free-flow wind speed estimation results using the local measurement of the second ($N = 1$ case) and, respectively, third ($N = 2$ case) turbine for a window of 10 minutes. The reference for the free-flow wind speed comes from experimental data. The gain is $k = 10$ and $\hat{U}_\infty(0) = 10$ m/s.

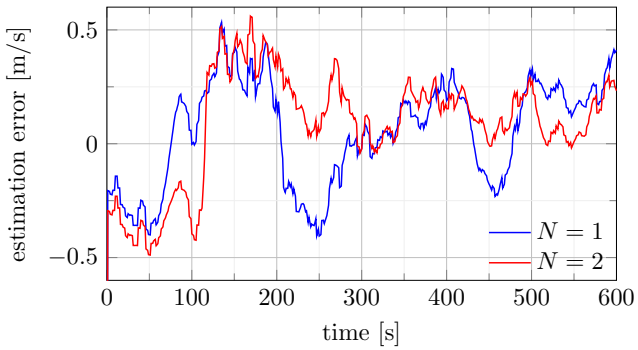

Fig. 3. Free-flow wind speed estimation error for the cases presented in Fig. 2.

The values of the coefficients κ_i and the induction factors were tuned on preliminary tests with known constant free-flow wind speed. The parameters selected were $a_1 = 0.27$, $a_2 = 0.32$, $\kappa_1 = 0.03$, and $\kappa_2 = 0.15$.

To achieve a more realistic test, we fed to FAST.Farm a free-flow wind speed that was obtained with experimental field data from a LiDAR mounted on an operating turbine. These LiDAR data were provided by Leosphere within the framework of the project SmartEole of the French National Research Agency (ANR).

Fig. 2 displays the estimation results in both the $N = 1$ and $N = 2$ cases. We used $k = 10$ and $\hat{U}_\infty(0) = 10$ m/s in both cases. The errors $U_\infty - \hat{U}_\infty$ for these same cases are depicted in Fig. 3.

Fig. 4 depicts the actual local measurement provided in the $N = 2$ case compared to one estimated by the model. We see that the measurement estimate converges very fast and thus, the estimation error observed in Fig. 2, which remains low enough, is due to the modeling error.

In Fig. 5, we use the same data in the $N = 2$ case, but we add noise to the measurements and show the effect of using different values for the gain k. We used $\hat{U}_\infty(0) = 10$ m/s as

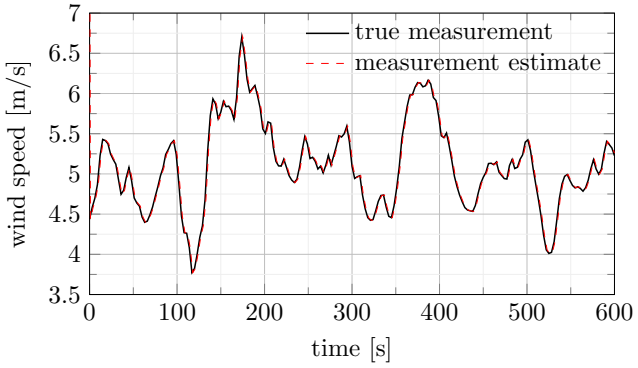

Fig. 4. Estimation of the local speed measurement in the $N = 2$ case corresponding to Fig. 2.

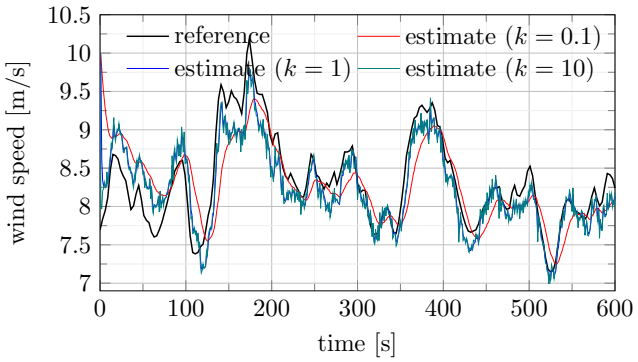

Fig. 5. Free-flow wind speed estimation results using noisy local measurements of the third turbine ($N = 2$) for different gains. We used $\hat{U}_\infty(0) = 10$ m/s.

before. At each measurement, the added noise is sampled from a zero-mean Gaussian distribution with a standard deviation equal to 2% of the true value of the measurement. One can observe some degradation of the performance, as one would expect, but the estimates still exhibit a similar trend to the actual wind speed. We also notice that the effect of the noise is less pronounced when a small gain ($k = 0.1$) is used, as one would expect for a technique that relies on output feedback, but at the expense of the time response.

IV. Conclusions

We presented a method for estimating the free-flow wind speed acting on an array of wind turbines using wind speed measurements that are affected by the wake of the array. The effectiveness of the method was tested using numerical simulations with data obtained from the FAST.Farm simulator. The presented method is simple to implement and possesses performance guarantees.

Although some idealizations were made (such as the turbines being placed so that they are aligned with the wind direction), this method provides interesting results using only a very simple wake model and could be implemented in real-time. This indicates it could be used as a building block for estimation strategies designed for more complex scenarios, such as when the wind direction is unknown and/or time-varying. Future works could go in this direction, using e.g., the 2-D extension [21] of the wake model used here that takes into account the wake deflection caused when there is a misalignment between the turbines and the wind direction. Another possible path for future research is trying to extend this method to identify other possibly unknown parameters (such as the wake expansion coefficients) of the wind farm.

Appendix
Proof of Theorem 1

The proof follows essentially the same steps as the one of [14, Theorem 1], but it was modified to account for the error term Δ in the measurement equation (9) and the fact that we may have $N > 1$ (i.e., multiple turbines causing the wake) here.

Let $V(t) \triangleq \tilde{U}_\infty^2(t)/2$ and $\delta\tilde{u}(t) \triangleq \delta\tilde{u}_1(t) + \ldots + \delta\tilde{u}_N(t)$. We have

$$\dot{V}(t) = \tilde{U}_\infty(t)\dot{\tilde{U}}_\infty(t) = \tilde{U}_\infty(t)(\dot{U}_\infty(t) - \dot{\hat{U}}_\infty(t)).$$

Notice that

$$\dot{\hat{U}}_\infty(t) = k(y(t) - \hat{y}(t)) = k(\tilde{U}_\infty(t) - \delta\tilde{u}(t) + \Delta(t)).$$

Using this and Assumptions 1 and 2, we have

$$\begin{aligned}\dot{V}(t) &\leq |\tilde{U}_\infty(t)|\zeta - k\tilde{U}_\infty^2(t) + k|\tilde{U}_\infty(t)||\delta\tilde{u}(t) + \Delta(t)| \\ &\leq |\tilde{U}_\infty(t)|\zeta - k\tilde{U}_\infty^2(t) + k|\tilde{U}_\infty(t)|\left(|\delta\tilde{u}(t)| + \Delta_M\right). \quad (22)\end{aligned}$$

The following inequality is shown in the proof of [14, Theorem 1] (and we suppress the details here for the sake of brevity)

$$|\delta\tilde{u}_i(t)| \leq \left(\alpha_i + \frac{\beta_i\zeta}{\hat{U}_m^2}\right) \sup_{s\in[-\bar{\tau},0]} |\tilde{U}_\infty(t+s)|.$$

Thus, it is clear that

$$|\delta\tilde{u}(t)| \leq Z \sup_{s\in[-\bar{\tau},0]} |\tilde{U}_\infty(t+s)|. \quad (23)$$

Recall that the constants α_i, β_i, and Z are defined in Assumption 3.

Combining (22) and (23), we see that

$$\begin{aligned}\dot{V}(t) &\leq |\tilde{U}_\infty(t)|(\zeta + k\Delta_M) - k\tilde{U}_\infty^2(t) \\ &\quad + kZ \sup_{s\in[-\bar{\tau},0]} \tilde{U}_\infty^2(t+s) \\ &\leq \sqrt{2V(t)}(\zeta + k\Delta_M) - 2kV(t) \\ &\quad + 2kZ \sup_{s\in[-\bar{\tau},0]} V(t+s).\end{aligned}$$

Then, from Young's inequality, we have that

$$\sqrt{2V(t)}(\zeta + k\Delta_M) \leq \frac{\epsilon(\zeta + k\Delta_M)^2}{2} + \frac{V(t)}{\epsilon}$$

for any $\epsilon > 0$. Defining $\rho = 2k\epsilon > 0$, we have

$$\begin{aligned}\dot{V}(t) &\leq \frac{\rho(\zeta + k\Delta_M)^2}{4k} - 2k\left(1 - \frac{1}{\rho}\right)V(t) \\ &\quad + 2kZ \sup_{s\in[-\bar{\tau},0]} V(t+s).\end{aligned}$$

Let us choose a value of ρ such that $Z < 1 - 1/\rho$. Then we can apply a generalization of Halanay's inequality [22] to show that there is a $\sigma_1 > 0$ such that

$$V(t) \leq \sup_{s\in[-\bar{\tau},0]} V(s)e^{-\sigma_1 t} + \frac{\rho(\zeta + k\Delta_M)^2}{8k^2\left(1 - \frac{1}{\rho} - Z\right)}.$$

Notice that such ρ exists if and only if Assumption 3 holds.

Finally, using the fact that $\sqrt{a^2+b^2} \leq |a| + |b|$, we have

$$\begin{aligned}|\tilde{U}_\infty(t)| &\leq \sqrt{2\sup_{s\in[-\bar{\tau},0]} V(s)e^{-\sigma_1 t} + \frac{\rho(\zeta + k\Delta_M)^2}{4k^2\left(1 - \frac{1}{\rho} - Z\right)}} \\ &\leq \sup_{s\in[-\bar{\tau},0]} |\tilde{U}_\infty(s)|e^{-\sigma t} + \frac{\sqrt{\rho}(\zeta + k\Delta_M)}{2k\sqrt{1 - \frac{1}{\rho} - Z}},\end{aligned}$$

where $\sigma = \sigma_1/2$. We minimize this upper bound by picking $\rho = 2/(1-Z)$, which yields (19).

To prove that $\hat{U}_\infty(t)$ remains lower-bounded, consider $\hat{U}_m \in (0, U_m - \Delta_M/(1-Z))$ and

$$k_* \triangleq \frac{\zeta/(1-Z)}{U_m - \hat{U}_m - \frac{\Delta_M}{1-Z} - \sup_{s\in[-\bar{\tau},0]}|\tilde{U}_\infty(s)|}.$$

Notice $k_* > 0$ because we assume in the statement of the theorem that $\sup_{s\in[-\bar{\tau},0]}|\tilde{U}_\infty(s)| < U_m - \hat{U}_m - \Delta_M/(1-Z)$. Also,

$$\hat{U}_\infty(0) = U_\infty(0) - \tilde{U}_\infty(0) \geq U_m - \sup_{s\in[-\bar{\tau},0]} |\tilde{U}_\infty(s)| > \hat{U}_m.$$

By way of contradiction, suppose there exists $t_1 > 0$ such that $\hat{U}_\infty(t_1) < \hat{U}_m$. Since $\hat{U}_\infty$ is continuous, there must be a $t_2 \in (0, t_1)$ such that $\hat{U}_\infty(t) > \hat{U}_m$ for all $t \in [0, t_2)$ and $\hat{U}_\infty(t_2) = \hat{U}_m$. Using (19) with $t = t_2$ and $k > k_*$, we have

$$\begin{aligned}|\tilde{U}_\infty(t_2)| &< \sup_{s\in[-\bar{\tau},0]} |\tilde{U}_\infty(s)|e^{-\sigma t_2} + \frac{\zeta}{k_*(1-Z)} + \frac{\Delta_M}{1-Z} \\ &\leq \sup_{s\in[-\bar{\tau},0]} |\tilde{U}_\infty(s)|e^{-\sigma t_2} + U_m - \hat{U}_m - \sup_{s\in[-\bar{\tau},0]} |\tilde{U}_\infty(s)| \\ &\leq U_m - \hat{U}_m - \sup_{s\in[-\bar{\tau},0]} |\tilde{U}_\infty(s)|\left(1 - e^{-\sigma t_2}\right).\end{aligned}$$

Then,

$$\begin{aligned}\hat{U}_\infty(t_2) &= U_\infty(t_2) - \tilde{U}_\infty(t_2) \geq U_m - |\tilde{U}_\infty(t_2)| \\ &> U_m - \left[U_m - \hat{U}_m - \sup_{s\in[-\bar{\tau},0]} |\tilde{U}_\infty(s)|\left(1 - e^{-\sigma t_2}\right)\right] \\ &\geq \hat{U}_m + \sup_{s\in[-\bar{\tau},0]} |\tilde{U}_\infty(s)|\left(1 - e^{-\sigma t_2}\right) \geq \hat{U}_m,\end{aligned}$$

i.e., $\hat{U}_\infty(t_2) > \hat{U}_m$. But, t_2 was defined so that $\hat{U}_\infty(t_2) = \hat{U}_m$, so this is a contradiction and therefore we cannot have a t_1 such that $\hat{U}_\infty(t_1) < \hat{U}_m$. This concludes the proof.

References

[1] C. R. Shapiro, P. Bauweraerts, J. Meyers, C. Meneveau, and D. F. Gayme, "Model-based receding horizon control of wind farms for secondary frequency regulation," *Wind Energy*, vol. 20, no. 7, pp. 1261–1275, 2017.

[2] J. Lee and F. Zhao, "Global Wind Report 2022," GWEC, Technical Report, April 2022. [Online]. Available: https://gwec.net/wp-content/uploads/2022/04/Annual-Wind-Report-2022_screen_final_April.pdf

[3] A. C. Kheirabadi and R. Nagamune, "A quantitative review of wind farm control with the objective of wind farm power maximization," *Journal of Wind Engineering and Industrial Aerodynamics*, vol. 192, pp. 45–73, 2019.

[4] L. E. Andersson, O. Anaya-Lara, J. O. Tande, K. O. Merz, and L. Imsland, "Wind farm control - Part I: A review on control system concepts and structures," *IET Renewable Power Generation*, vol. 15, no. 10, pp. 2085–2108, 2021.

[5] T. Knudsen, T. Bak, and M. Svenstrup, "Survey of wind farm control—power and fatigue optimization," *Wind Energy*, vol. 18, no. 8, pp. 1333–1351, 2015.

[6] L. Y. Pao and K. E. Johnson, "A tutorial on the dynamics and control of wind turbines and wind farms," in *2009 American Control Conference*. IEEE, 2009, pp. 2076–2089.

[7] K. E. Johnson and N. Thomas, "Wind farm control: Addressing the aerodynamic interaction among wind turbines," in *2009 American Control Conference*. IEEE, 2009, pp. 2104–2109.

[8] T. G. Bozkurt, G. Giebel, N. K. Poulsen, and M. Mirzaei, "Wind speed estimation and parametrization of wake models for downregulated offshore wind farms within the scope of PossPOW project," in *Journal of Physics: Conference Series*, vol. 524, no. 1. IOP Publishing, 2014, p. 012156.

[9] F. Guillemin, H.-N. Nguyen, G. Sabiron, D. Di Domenico, and M. Boquet, "Real-time three dimensional wind field reconstruction from nacelle LiDAR measurements," in *Journal of Physics: Conference Series*, vol. 1037, no. 3. IOP Publishing, 2018, p. 032037.

[10] E. Simley, L. Pao, N. Kelley, B. Jonkman, and R. Frehlich, "Lidar wind speed measurements of evolving wind fields," in *50th AIAA aerospace sciences meeting including the new horizons forum and aerospace exposition*, 2012, p. 656.

[11] J. M. Jonkman, J. Annoni, G. Hayman, B. Jonkman, and A. Purkayastha, "Development of FAST.Farm: A new multi-physics engineering tool for wind-farm design and analysis," in *35th Wind Energy Symposium*, 2017.

[12] J. M. Jonkman and K. Shaler, *FAST.Farm user's guide and theory manual*. National Renewable Energy Laboratory Golden, CO, 2021. [Online]. Available: https://www.nrel.gov/docs/fy21osti/78485.pdf

[13] C. R. Shapiro, J. Meyers, C. Meneveau, and D. F. Gayme, "Dynamic wake modeling and state estimation for improved model-based receding horizon control of wind farms," in *2017 American Control Conference (ACC)*. IEEE, 2017, pp. 709–716.

[14] E. B. R. F. Paiva, O. Lepreux, and D. Bresch-Pietri, "Transport speed estimation for a 1-D hyperbolic PDE based on output flow measurement," in *2022 10th International Conference on Systems and Control (ICSC)*. IEEE, 2022, pp. 72–77.

[15] D. Bresch-Pietri and N. Petit, "Implicit integral equations for modeling systems with a transport delay," in *Recent Results on Time-Delay Systems*. Springer, 2016, pp. 3–21.

[16] C.-H. Clerget and N. Petit, "Optimal control of systems subject to input-dependent hydraulic delays," *IEEE Transactions on Automatic Control*, vol. 66, no. 1, pp. 245–260, 2020.

[17] M. F. Howland and J. O. Dabiri, "Influence of wake model superposition and secondary steering on model-based wake steering control with SCADA data assimilation," *Energies*, vol. 14, no. 1, 2021. [Online]. Available: https://www.mdpi.com/1996-1073/14/1/52

[18] H. Zong and F. Porté-Agel, "A momentum-conserving wake superposition method for wind farm power prediction," *Journal of Fluid Mechanics*, vol. 889, 2020.

[19] T. Göçmen, P. Van der Laan, P.-E. Réthoré, A. P. Diaz, G. C. Larsen, and S. Ott, "Wind turbine wake models developed at the technical university of Denmark: A review," *Renewable and Sustainable Energy Reviews*, vol. 60, pp. 752–769, 2016.

[20] F. Porté-Agel, M. Bastankhah, and S. Shamsoddin, "Wind-turbine and wind-farm flows: a review," *Boundary-Layer Meteorology*, vol. 174, no. 1, pp. 1–59, 2020.

[21] C. R. Shapiro, D. F. Gayme, and C. Meneveau, "Modelling yawed wind turbine wakes: a lifting line approach," *Journal of Fluid Mechanics*, vol. 841, 2018.

[22] H. Wen, S. Shu, and L. Wen, "A new generalization of Halanay-type inequality and its applications," *Journal of Inequalities and Applications*, vol. 2018, no. 1, pp. 1–12, 2018.